symmetry

MDPI

Article

Lump-Type Solutions, Mixed Solutions and Rogue Waves for a (3+1)-Dimensional Variable-Coefficients Burgers Equation

Jianwen Wu [1], Yuejin Cai [2,3] and Xueping Cheng [4,*]

[1] Department of Mathematics and Physics, Quzhou University, Quzhou 324000, China; wujw361@qzc.edu.cn
[2] Department of Physics, Zhejiang Normal University, Jinghua 321004, China; caiyj@aqnu.edu.cn
[3] School of Computer and Information, Anqing Normal University, Anqing 246133, China
[4] School of Science, Zhejiang University of Science and Technology, Hangzhou 310023, China
* Correspondence: chengxp2005@126.com

Abstract: In this work, we consider the (3+1)-dimensional Burgers equation with variable coefficients, which is frequently used to define the motion of solitary waves. Abundant lump waves are constructed by taking the ansatz as a rational function. Furthermore, mixed solutions utilizing lump waves, rogue waves, and kink solitons are obtained by combining the rational function with an exponential function, resulting in fission and fusion phenomena.

Keywords: variable-coefficients Burgers equation; lump solutions; lump soliton solutions; rogue waves

check for updates

Citation: Wu, J.; Cai, Y.; Cheng, X. Lump-Type Solutions, Mixed Solutions and Rogue Waves for a (3+1)-Dimensional Variable-Coefficients Burgers Equation. *Symmetry* **2024**, *16*, 779. https://doi.org/10.3390/sym16070779

Academic Editor: Junesang Choi

Received: 20 May 2024
Revised: 9 June 2024
Accepted: 18 June 2024
Published: 21 June 2024

1. Introduction

Nonlinear evolution equations (NLEEs) have gained increasing attention in the field of nonlinear science due to their many applications in various fields, such as fluid mechanics [1,2], plasma physics [3], optics [4], biology [5], and condensed matter physics [6]. The most important of these studies are meant to obtain soliton solutions. Many methods have been developed, including the inverse scattering transformation [7,8], the Darboux transformation [9], Bäcklund transformations [10], and Hirota's bilinear technique [11].

The lump waves in the Kadomtsev–Petviashvili (KP) equation were theoretically predicted using the long wave limit approach [12]. This type of solution was observed in optical fibers [13], which attracted the attention of researchers. Then, a symbolic computation approach was proposed to construct additional lump wave solutions of NLEEs, which was successfully used in the KP equation [14], the BKP-Korteweg de-Vries (BKP-KdV) equation [15], the KP3-4 equation [16], the higher-order KdV-5 equation [17], and many more [18–21]. Furthermore, M-lump solutions were constructed by making some parameters conjugate to each other [22]. The mixed lump wave solutions of the (2+1)-dimensional Sawada–Kotera equation were obtained by an ingenious limit approach [23]. In addition, interesting research on lump waves, higher-order lump waves, and the interaction between waves was conducted using the ansatz method, such as the spatial symmetric (2+1)-dimensional dispersive wave model [24] and the (2+1)-dimensional Mel'nikov equation [25]. Compared to the version of NLEEs with constant coefficients, the one with variable coefficients can obtain a larger number of new solutions for complex physical models and describe realistic physical phenomena [26]. An example of this is the variable-coefficients, high-order, nonlinear Schrödinger equation (VcHNLS). By using reductive perturbation theory with long wave approximation, VcHNLS can be used to study the propagation of pulse waves in deformable elastic vessels filled with inviscid blood [27].

Burgers-type equations are frequently used to define the motion of solitary waves in many fields, such as ocean dynamics [28], vehicular traffic [29], and particle systems [30]. Recently, more exact solutions to Burgers-type equations have been constructed by various methods, such as the nonlocal symmetry group reduction method [31], the consistent tanh expansion method [32], and the velocity resonance method [33]. In Ref. [34], soliton-like and period-form solutions were gained using the extended tanh method. Based on the ansatz method, lump solutions and period lump solutions were constructed in Ref. [35]. Two types of semi-rational solutions were unearthed for the constant-coefficient (3+1)-dimensional Burgers equation [36]. By means of the test function method, lump waves and mixed solutions were constructed for the generalized (2+1) Burgers equation with variable coefficients [37]. In addition, by using white noise analysis, Hermite transformation of the solitary wave solutions of the Wick-type stochastic Burgers equation (WSB) were discussed, which evolved the density field of the weakly asymmetric exclusion process. The WSB is of the form

$$U_t + p(t)(U_{xx} + U\diamondsuit U_x) = W(t)\diamondsuit R^{\diamondsuit}(t, U, U_x, U_{xx}), \tag{1}$$

which is the perturbation of the Burgers equation with variable coefficients

$$u_t + p(t)(u_{xx} + uu_x) = 0. \tag{2}$$

Here, $p(t)$ is a function of t, $W(t)$ defines the Gaussian white noise, and "$\diamondsuit$" denotes the Wick production in the Kondratiev distribution space [38]. Motivated by the above scientific applications, the aim of this paper is to investigate additional new solutions to a (3+1)-dimensional variable-coefficients Burgers equation (VcB):

$$\begin{aligned} &u_y + m(t)u_x + n(t)u_z + p(t)(u_{xx} + 2vu_x) \\ &\quad + q(t)(u_{yy} + 2uu_y) + r(t)(u_{zz} + 2wu_z) + s(t)u_t = 0, \\ &u_x = v_y, u_z = w_y, \end{aligned} \tag{3}$$

with real functions $u = u(x, y, z, t)$, $v = v(x, y, z, t)$, and $w = w(x, y, z, t)$, while m, n, p, q, r, and s are any real functions with respect to time-independent variable t. However, mixed lump waves and solitons and rogue waves of VcB (3) have not yet been found.

The structure of this paper is as follows: Rational solutions are found by means of the ansatz technique in Section 2. Section 3 is aimed at finding solutions to the interaction between lump waves and multi-kink solitons. The details of the effects of the ansatz function are provided, and some special types of interactions are unearthed, such as fission, fusion, and rogue wave phenomena. Section 4 consists of discussion, some features, and comments. It should be noted that the graphical representation of the solution was provided by Maple.

2. Rational Solution of the (3+1)-Dimensional Variable-Coefficients Burgers Equation

An effective method for solving a PDE is to use the Hirota method [11]. In this section, by means of this method, we seek the rational solution for VcB (3), and the first thing to do is to use the following dependent variable transformation:

$$u = (\ln f)_y, \quad v = (\ln f)_x, \quad w = (\ln f)_z, \tag{4}$$

and to rewrite VcB (3) in the following bilinear form:

$$\begin{aligned} &f_y^2 - ff_{yy} + m(t)(ff_{xy} - f_x f_y) + n(t)(ff_{yz} - f_y f_z) + p(t)(ff_{xxy} - f_{xx} f_y) \\ &\quad + q(t)(ff_{yyy} - f_y f_{yy}) + r(t)(ff_{yzz} - f_y f_{zz}) + s(t)(f_y f_t - ff_{yt}) = 0, \end{aligned} \tag{5}$$

where f is a real function. In order to obtain the rational solution of VcB (3), we assume that f has the following form:

$$f = \xi^2 + \phi^2 + a_9, \tag{6}$$

with $\xi(x,y,z,t) = a_1x + a_2y + a_3z + a_4(t)$ and $\phi(x,y,z,t) = a_5x + a_6y + a_7z + a_8(t)$, where $a_4(t)$ and $a_8(t)$ are any real functions related to t and a_i $(i = 1,\ 2,\ \cdots,\ 9)$ are arbitrary real parameters. Substituting Equation (6) into Equation (5) and vanishing all the coefficients of x, y, z, and t, the relations among arbitrary constants are obtained as

$$\begin{aligned} p(t) &= -\frac{q(t)(a_2^2 + a_6^2)}{a_1^2 + a_5^2} - \frac{r(t)(a_3^2 + a_7^2)}{a_1^2 + a_5^2}, \\ s(t) &= \frac{m(t)(a_1a_7 - a_3a_5) + a_2a_7 - a_6a_3}{a_7a_4(t)' - a_3a_8(t)'}, \\ n(t) &= \frac{m(t)[a_1a_8(t)' - a_5a_4(t)'] + a_2a_8(t)' - a_6a_4(t)'}{a_7a_4(t)' - a_3a_8(t)'}, \end{aligned} \tag{7}$$

where $a_8(t)' \equiv \frac{\mathrm{d}a_8(t)}{\mathrm{d}t}$ references the derivative of $a_8(t)$ about t. Substituting Equations (6) and (7) into the transformation $u = (\ln f)_y$, the exact solution is written as

$$u = (\ln f)_y = 2\frac{(a_1a_2 + a_5a_6)x + (a_2^2 + a_6^2)y + (a_2a_3 + a_6a_7)z + a_4(t)a_2 + a_8(t)a_6}{[a_1x + a_2y + a_3z + a_4(t)]^2 + [a_5x + a_6y + a_7z + a_8(t)]^2 + a_9}. \tag{8}$$

Here, we obtain two kinds of lump wave.

Example 1. *When $a_4(t) = t$, $a_8(t) = 3t + 4$, $m(t) = t^2$, $r(t) = -t$, $a_1 = 8$, $a_2 = 1$, $a_3 = 0.2$, $a_5 = a_7 = 2$, $a_6 = 0.01$, and $a_9 = 4$, their spatial structure and the propagation of the lump of u are described in Figure 1 at $t = -25$, $t = 0$, and $t = 25$.*

According to Figure 1, it can be found that the lump wave moves in the positive direction of the y axis and the negative direction of the z axis. Figure 1a is the three-dimensional image of the lump solution, which shows the spatial structure with a peak and a trough, and the solution decays in all spatial directions.

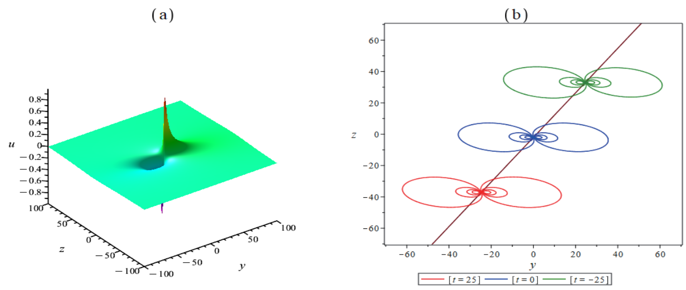

Figure 1. The propagations of the lump wave, u, given by Equation (8) in Example 1: (**a**) The three-dimensional structure plot at $t = 0$; (**b**) The evolution plot of $t = -25,\ 0,\ 25$, with the red line indicating the movement track of the lump.

Example 2. *When $a_4(t) = e^{\frac{t}{4}}$, $a_8(t) = e^{\frac{t}{4}}$, $m(t) = -t$, $r(t) = t$, $a_1 = a_6 = 1$, $a_2 = 4$, $a_3 = a_5 = a_7 = 2$, and $a_9 = 4$, the three-dimensional structure plots of the lump wave solution are obtained, and it is obvious that when $t < 0$, the lump wave remains stationary. On the contrary, when $t > 0$, the lump wave starts to move, and with the increase of t, the lump wave quickly moves away from the initial position. The lump wave solution is stable when it exists alone. Could the lump wave maintain its properties after colliding with solitons or other nonlinear waves? Next, we will discuss the interaction between solitons and lump waves below.*

3. Interaction between Solitons and Lump Waves

In the following section, we focus on constructing the interaction solutions between lump waves and solitons by combining the rational functions and exponential functions.

First of all, we take the function f as the ansatz with the following rational–exponential function:

$$f = \xi^2 + \phi^2 + a_9 + \lambda_1(t)e^{\phi_1 x+\phi_2 y+\phi_3 z+\phi_4(t)} + \lambda_2(t)e^{-\phi_1 x-\phi_2 y-\phi_3 z-\phi_4(t)}, \tag{9}$$

with $\xi(x,y,z,t) = a_1x + a_2y + a_3z + a_4(t)$ and $\phi(x,y,z,t) = a_5x + a_6y + a_7z + a_8(t)$, where $a_4(t)$, $a_8(t)$, and $\phi_4(t)$ are any real functions related to t, and the parameters a_i $(i = 1, 2, \cdots, 9)$ and ϕ_i $(i = 1, 2, 3)$ are determined real parameters. By substituting Equation (9) into Equation (5) and vanishing the different powers of the variables x, y, z, and t, we obtain a series of algebraic equations on the undetermined parameters. We will discuss two cases questioning whether $\lambda_1(t)$ is equal to zero, and the same number of cases questioning whether $\lambda_2(t)$ is zero is similar to that not discussed here.

Case 1: $\lambda_1(t) = 0$

After solving these algebraic equations, a set of constraining relations is obtained as follows:

$$\begin{aligned}
s(t) &= \frac{m(t)(a_3a_5 - a_1a_7) + a_3a_6 - a_2a_7}{a_3a_8(t)'},\ q(t) = -\frac{(a_1^2+a_5^2)p(t)}{a_2^2+a_6^2} - \frac{(a_3^2+a_7^2)r(t)}{a_2^2+a_6^2},\\
\lambda_2(t) &= c_1 \exp\Big[\int \frac{g_1}{(a_2^2+a_6^2)(a_1a_7m(t) - a_3a_5m(t) + a_2a_7 - a_3a_6)}\mathrm{d}t\Big],\\
g_1 &= (a_2^2+a_6^2)[(a_8(t)'\phi_1 - a_5\phi_4(t)')a_3 + (a_7\phi_4(t)' - a_8(t)'\phi_3)a_1]m(t)\\
&\quad + a_3^3a_8(t)'\phi_2^2r(t) + [\phi_2^2a_7^2a_8(t)'r(t) + (\phi_2 - \phi_3^2r(t))a_2^2a_8(t)'\\
&\quad + (\phi_2 - \phi_3^2r(t))a_6^2a_8(t)']a_3 + a_2(a_2^2+a_6^2)(a_7\phi_4(t)' - a_8(t)'\phi_3),\\
&\quad - [\phi_1^2(a_2^2+a_6^2) - \phi_2^2(a_1^2+2a_5^2)]a_8(t)'a_3,\\
n(t) &= -\frac{a_1m(t)+a_2}{a_3},\ \lambda_1(t) = 0,\ a_4(t) = c_2,
\end{aligned} \tag{10}$$

with the integral constant c_1. The interaction solution between the lump wave and the soliton of the (3+1)-dimensional VcB is constructed:

$$u = 2(\ln f)_y = \frac{4a_2\xi + 4a_6\phi - 2\phi_2c_1l_1}{\xi^2+\phi^2+c_1l_1+a_9}, \tag{11}$$

where

$$\begin{aligned}
&\xi = a_1x + a_2y + a_3z + c_2,\ \phi = a_5x + a_6y + a_7z + a_8(t),\\
&l_1 = \exp\Big[\int \frac{g_1}{(a_3^2+a_7^2)(a_1a_7m(t) - a_3a_5m(t) + a_2a_7 - a_3a_6)}\mathrm{d}t\Big]e^{-\phi_1x-\phi_2y-\phi_3z-\phi_4(t)}.
\end{aligned} \tag{12}$$

Example 3. *When the parameters are selected as*

$$\begin{aligned}
&a_1 = 8,\ a_2 = c_2 = \phi_3 = 1,\ a_3 = \frac{1}{5},\ a_5 = a_7 = c_1 = 2,\ a_6 = \frac{1}{100},\ a_9 = 4,\\
&\phi_1 = \phi_2 = \frac{1}{2},\ r(t) = t,\ a_8(t) = 3t+3,\ m(t) = \frac{1}{2t^2},\ p(t) = \frac{1}{10},\ \phi_4(t) = t.
\end{aligned} \tag{13}$$

The solution utilizing an interaction between a kink wave and a lump wave is obtained as shown in Figure 2. Figure 2a–c show the three-dimensional plot at $t = -50$, $t = 0$, and $t = 200$, respectively. According to the figures, it is found that the speed of the kink soliton is greater than that of the lump wave and that the kink soliton can catch up with the lump wave in this time period. In the process of interaction, the amplitude of the lump wave becomes smaller and smaller until the lump wave is completely engulfed and continues to spread. The convergence phenomenon of kink solitons and lump waves is observed.

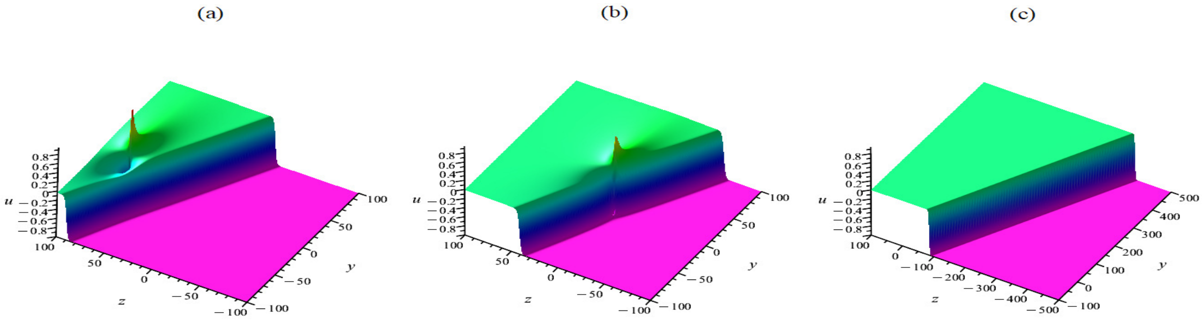

Figure 2. The mixed solution utilizing kink soliton and lump waves. (**a**–**c**) The three-dimensional plots of $t=-50$, $t=0$, and $t=200$.

Case 2: $\lambda_1(t) \neq 0$

By the same operation, the solution of the interaction between a soliton and a lump wave is obtained as

$$u = 2(\ln f)_y = \frac{4a_2\xi + 4a_6\phi + 2\phi_2(c_1 l_1 - c_2 l_2)}{\xi^2 + \phi^2 + c_1 l_1 + a_9}, \tag{14}$$

where

$$\begin{aligned}
&\xi = a_1 x + a_2 y + a_3 z + a_4(t),\ \phi = a_5 x + a_6 y + a_7 z + a_8(t),\\
&l_1 = \exp\Big[\int \frac{-g_1}{(a_3^2+a_7^2)(a_1a_7m(t) - a_3a_5m(t) + a_2a_7 - a_3a_6)}\mathrm{d}t\Big] e^{\phi_1 x + \phi_2 y + \phi_3 z + \phi_4(t)},\\
&l_2 = \exp\Big[\int \frac{g_2}{(a_3^2+a_7^2)(a_1a_7m(t) - a_3a_5m(t) + a_2a_7 - a_3a_6)}\mathrm{d}t\Big] e^{-\phi_1 x - \phi_2 y - \phi_3 z - \phi_4(t)}.
\end{aligned} \tag{15}$$

The corresponding parameters satisfy the following requirements:

$$\begin{aligned}
s(t) &= \frac{m(t)(a_3a_5 - a_1a_7) + a_3a_6 - a_2a_7}{a_3a_8(t)'},\ q(t) = -\frac{(a_1^2+a_5^2)p(t)}{a_2^2+a_6^2} - \frac{(a_3^2+a_7^2)r(t)}{a_2^2+a_6^2},\\
\lambda_1(t) &= c_1 \exp\Big[\int \frac{-g_1}{(a_2^2+a_6^2)(a_1a_7m(t) - a_3a_5m(t) + a_2a_7 - a_3a_6)}\mathrm{d}t\Big],\\
g_1 &= (a_2^2+a_6^2)[a_3\phi_1^2 p(t) + a_3\phi_3^2 r(t) - a_1\phi_3 m(t) + a_3\phi_1 m(t) - a_2\phi_3\\
&\quad + a_3\phi_2]a_8(t)' - a_3\phi_2^2[(a_1^2+a_5^2)p(t) + (a_3^2 r + a_7^2)r(t)]a_8(t)'\\
&\quad + (a_2^2+a_6^2)[a_1a_7m(t) - a_3a_5m(t) + a_2a_7 - a_3a_6]\phi_4(t)',\\
\lambda_2(t) &= c_2 \exp\Big[\int \frac{g_2}{(a_2^2+a_6^2)(a_1a_7m(t) - a_3a_5m(t) + a_2a_7 - a_3a_6)}\mathrm{d}t\Big],\\
g_2 &= -(a_2^2+a_6^2)[a_3\phi_1^2 p(t) + a_3\phi_3^2 r(t) + a_1\phi_3 m(t) - a_3\phi_1 m(t) + a_2\phi_3\\
&\quad - a_3\phi_2]a_8(t)' + a_3\phi_2^2[(a_1^2+a_5^2)p(t) + (a_3^2 r + a_7^2)r(t)]a_8(t)'\\
&\quad + (a_2^2+a_6^2)[a_1a_7m(t) - a_3a_5m(t) + a_2a_7 - a_3a_6]\phi_4(t)',\\
n(t) &= -\frac{a_1 m(t) + a_2}{a_3},\ a_4(t) = c_3.
\end{aligned} \tag{16}$$

Here, we obtain two different forms by taking $m(t)$ as $\frac{2}{t^2}$ and e^t, and when $m(t)$ is taken to the non-even power of t, the solution will have singularity, which will not be discussed.

Example 4. *The appropriate parameters are selected as*

$$a_3 = a_5 = a_7 = c_1 = c_3 = p(t) = 2,\ a_1 = 8,\ \phi_1 = \phi_2 = \frac{1}{2},\ c_2 = \phi_3 = 1,$$
$$a_2 = a_9 = 4,\ a_6 = 0.01,\ a_8(t) = 3t + 4,\ q(t) = r(t) = \phi_4(t) = t,\ m(t) = \frac{2}{t^2}. \tag{17}$$

Then, the corresponding interaction solution between two kink solitons and a lump wave can be described by Figure 3a–e. We find that the two kink waves keep moving in opposite directions along the z axis. When $t < 0$, the lump wave appears between the two kink solitons, and the two kink solitons gradually swallow the lump wave until there are only two kink solitons in the space at $t > 0$. Finally, the lump wave gradually appears between the two kink waves. The density plot in Figure 3f shows that the lump wave disappears completely between the two kink solitons at $t = 0$. After the interaction between the lump wave and the soliton, the amplitudes, shapes, and velocities remain unchanged.

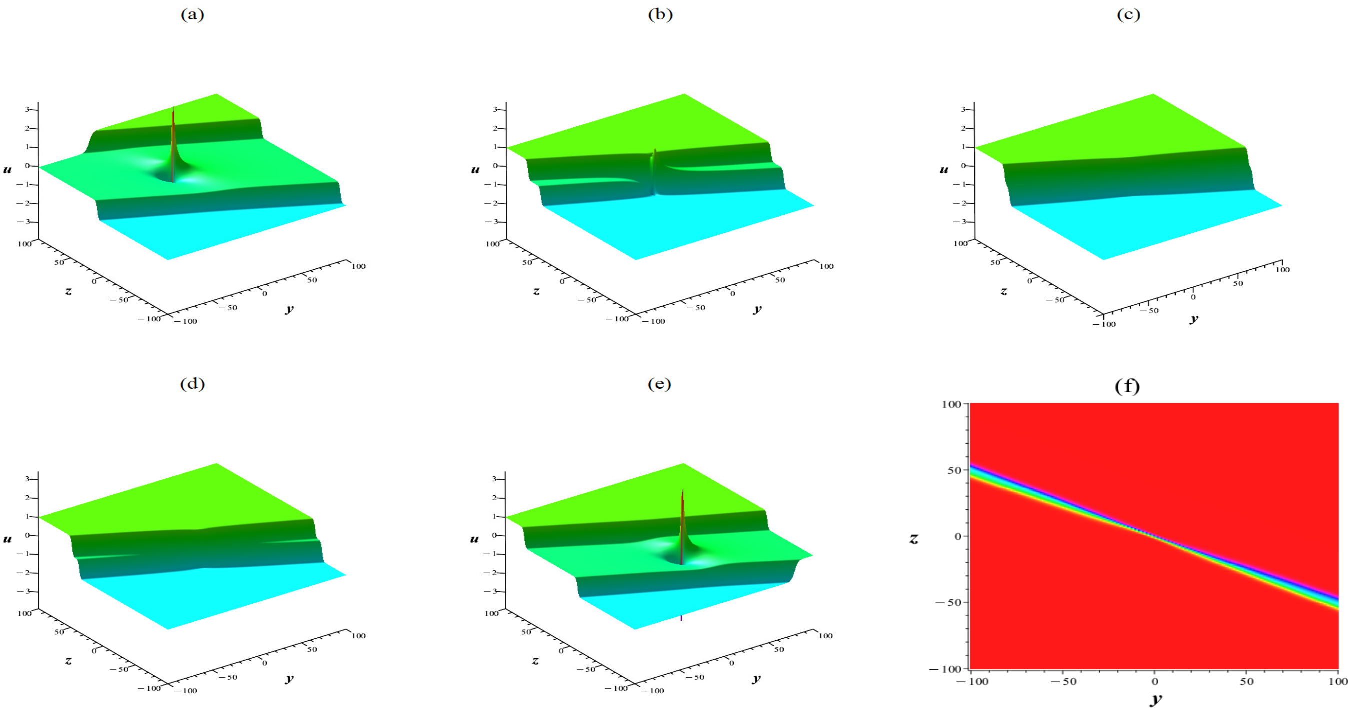

Figure 3. The solution for the interaction between two kink solitons and a lump wave: (**a**–**e**) the three-dimensional plots at $t = -35$, $t = -5$, $t = 0$, $t = 5$, and $t = 35$. (**f**) The density plots at $t = 0$.

Example 5. *We select the parameters as*

$$a_3 = a_5 = a_7 = c_1 = c_3 = p(t) = 2,\ a_1 = 8,\ \phi_1 = \phi_2 = \frac{1}{2},\ c_2 = \phi_3 = 1,$$
$$a_2 = a_9 = 4,\ a_6 = -1,\ a_8(t) = 3t + 4,\ q(t) = r(t) = \phi_4(t) = t,\ m(t) = e^t. \tag{18}$$

The interaction solution for two kink solitons and a lump wave is obtained, and the dynamic behavior of the solution is shown in Figure 4. As shown in Figure 4a–c, the three-dimensional plots of the interaction between two kink solitons and a lump wave are presented at $x = -10$, $x = 0$, and $x = 30$, respectively. It can be found that two kink waves move in the same direction with the same velocity along the negative direction of the z axis. When $x < 0$, the lump wave gradually appears between the two kink waves, and when $x > 0$, the two kink solitons gradually swallow the lump wave until there are only two kink solitons in the space, that is, the phenomenon of splitting occurs first, followed by converging. The phenomenon of the splitting and then polymerizing of two solitons and a lump wave also exists in the (3+1)-dimensional constant coefficient Burgers equation [35] *and other (3+1)-dimensional nonlinear systems [39]. For the variable-coefficients equation, when the appropriate parameters are utilized, the subsequent phenomena of first the convergence and then the splitting of two solitons and a lump wave can be obtained.*

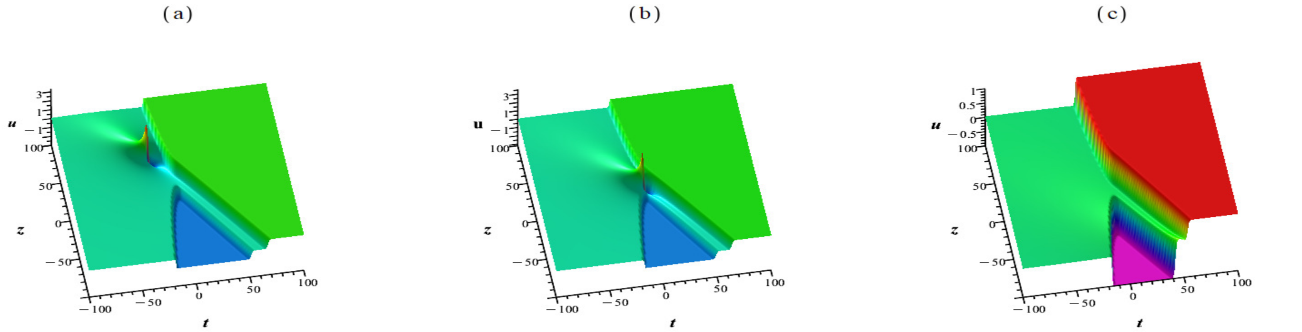

Figure 4. The interaction between two kink solitons and a lump wave. (**a**–**c**) The three-dimensional plots at $x = -10$, $x = 0$, and $x = 30$.

Example 6. *In this section, we attempt to reveal the rogue wave excited by the two kink solitons for a VcB (3). Let*

$$u = 2(\ln f)_y = \frac{4a_2\xi + 4a_6\phi + 2\phi_2(c_1 l_1 - c_2 l_2)}{\xi^2 + \phi^2 + c_1 l_1 + a_9}, \tag{19}$$

where

$$\begin{aligned} &\xi = a_1 x + a_2 y + a_3 z + c_3,\ \phi = a_5 x + a_6 y + a_7 z + a_8(t), \\ &l_1 = \exp\left[\int \frac{-g_1}{(a_3^2 + a_7^2)(a_1 a_7 m(t) - a_3 a_5 m(t) + a_2 a_7 - a_3 a_6)} \mathrm{d}t\right] e^{\phi_1 x + \phi_2 y + \phi_3 z + \phi_4(t)}, \\ &l_2 = \exp\left[\int \frac{g_2}{(a_3^2 + a_7^2)(a_1 a_7 m(t) - a_3 a_5 m(t) + a_2 a_7 - a_3 a_6)} \mathrm{d}t\right] e^{-\phi_1 x - \phi_2 y - \phi_3 z - \phi_4(t)}. \end{aligned} \tag{20}$$

The corresponding parameters satisfy the following requirements:

$$\begin{aligned} &a_3 = a_5 = a_7 = c_1 = c_3 = p(t) = 2,\ a_1 = 8,\ \phi_1 = \phi_2 = \frac{1}{2},\ c_2 = \phi_3 = 1, \\ &a_2 = a_9 = 4,\ a_6 = -1,\ a_8(t) = sin(t) + 4,\ q(t) = r(t) = \phi_4(t) = t,\ m(t) = t^2 + 6. \end{aligned} \tag{21}$$

*As seen in Figure 5, Equation (19) is a rogue wave excited by two kink solitons. Figure 5*d *shows that a rogue wave generates at $x = 0$, and the middle fold of the kink soliton becomes higher than before.*

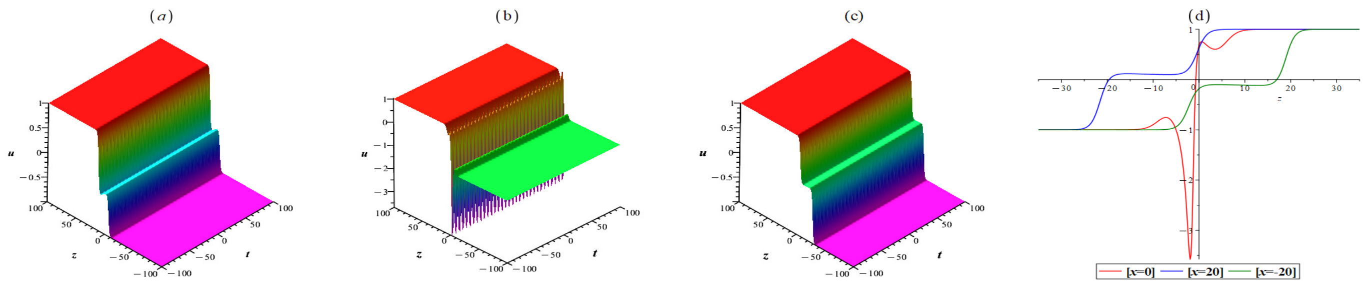

Figure 5. The rogue wave with two solitons. (**a**–**c**) The three-dimensional plots at $x = -20$, $x = 0$, and $x = 20$. (**d**) The evolution plot of $x = -20,\ 0,\ 20$.

4. Discussion

In this paper, a (3+1)-dimensional variable-coefficients Burgers equation (3) has been investigated, evolving from a bilinear form. Rational and rational–exponential solutions have been constructed via the direct ansatz method. By choosing the arbitrary functions suitably, the solutions involving rational and rational–exponential functions become lump waves and lump–kink waves, respectively. Based on a deep study, the lump solution driven by the bilinear form is a stable peak as the time increases, and the fission and fusion phenomena between soliton and lump waves have been discussed. Moreover, we attained a lump wave excited by two kink solitons. Finally, our study is not restricted to water rogue waves [40,41], but is also evident among rogue waves excited by two kink solitons. It may be applied to hydrodynamics and particle systems.

Author Contributions: The authors made equal contributions to this work, with special involvements as follows: Software, Y.C.; writing—original draft preparation, J.W.; writing—review and editing, X.C. All authors have read and agreed to the published version of the manuscript.

Funding: This research was funded by the National Natural Science Foundation of China (Grant Nos. 11975204 and 12075208).

Data Availability Statement: All data included in this study are available upon request by contacting the corresponding author.

Conflicts of Interest: The authors declare no conflicts of interest.

References

1. Joseph, R.I. Solitary waves in a finite depth fluid. *J. Phys. A Math. Gen.* **1977**, *10*, L225–L227. [CrossRef]
2. Barna, I.F.; Pocsai, M.A.; Mátyás, L. Time-dependent analytic solutions for water waves above sea of varying depths. *Mathematics* **2022**, *10*, 2311. [CrossRef]
3. Das, G.C.; Sarma, J.; Uberoi, C. Explosion of soliton in a multicomponent plasma. *Phys. Plasmas* **1997**, *4*, 2095. [CrossRef]
4. Polanco Adames, D.A.; Dou, J.P.; Lin, J.; Zhu, G.J.; Li, H.J. Nonlinear optical potential with Parity-Time symmetry in a coherent atomic gas. *Symmetry* **2022**, *14*, 1135. [CrossRef]
5. Chen, Z.M.; Duan, W.S. Rouge waves in fluid-filled elastic tube. *Acta. Phys. Sin.* **2020**, *69*, 014701. [CrossRef]
6. Wang, T.Y.; Zhou, Q.; Liu, W.J. Soliton fusion and fission for the high-order coupled nonlinear Schrödinger system in fiber lasers. *Chin. Phys. B* **2022**, *31*, 020501. [CrossRef]
7. Chen, M.; Fan, E.G. Riemann–Hilbert approach for discrete sine-Gordon equation with simple and double poles. *Stud. Appl. Math.* **2022**, *148*, 1180–1207. [CrossRef]
8. Hu, B.B.; Lin, J.; Zhang, L. Riemann–Hilbert problem associated with the vector Lakshmanan–Porsezian–Daniel model in the birefringent optical fibers. *Math. Method Appl. Sci.* **2022**, *45*, 11545–11561. [CrossRef]
9. Shi, X.R.; Yang, Y.Q. Exact solutions and Darboux transformation for the reverse space-time nonlocal Lakshmanan–Porsezian–Daniel equation. *Wave Motion* **2023**, *119*, 103141. [CrossRef]
10. Wang, G.H.; Liu, Q.P.; Mao, H. The modified Camassa–Holm equation: Bäcklund transformation and nonlinear superposition formula. *J. Phys. A Math. Theor.* **2020**, *53*, 294003. [CrossRef]
11. Hirota, R. *The Direct Method in Soliton Theory*; Cambridge University Press: Cambridge, UK, 2004.
12. Satsuma, J.; Ablowitz, M.J. Two-dimensional lumps in nonlinear dispersive systems. *J. Math. Phys.* **1979**, *20*, 1496–1503. [CrossRef]
13. Baronio, F.; Wabnitz, S.; Kodama, Y. Optical Kerr spatiotemporal dark-lump dynamics of hydrodynamic origin. *Phys. Rev. Lett.* **2016**, *116*, 173901. [CrossRef]
14. Zhang, Z.; Yang, X.Y.; Li, W.T.; Li, B. Trajectory equation of a lump before and after collision with line, lump, and breather waves for (2+1)-dimensional Kadomtsev–Petviashvili equation. *Chin. Phys. B* **2019**, *28*, 110201. [CrossRef]
15. Wu, H.L.; Wu, H.Y.; Zhu, Q.Y.; Fei, J.X.; Ma, Z.Y. Soliton, breather and lump molecules in the (2+1)-dimensional B-type Kadomtsev-Petviashvili-Korteweg De-Vries equation. *Appl. Anal. Comput.* **2022**, *12*, 230–244. [CrossRef]
16. Hao, X.Z.; Li, Y. Interaction phenomena between solitons, lumps and breathers for the combined KP3-4 equation. *Nonlinear Dyn.* **2023**, *111*, 6701–6710. [CrossRef]
17. Alshammari, F.S.; Rahman, Z.; Roshid, H.O.; Ullah, M.S.; Aldurayhim, A.; Ali, M.Z. Dynamical structures of multi-solitons and interaction of solitons to the higher-order KdV-5 equation. *Symmetry* **2023**, *15*, 626. [CrossRef]
18. Ma, H.C.; Mao, X.; Deng, A.P. Interaction solutions for the second extended (3+1)-dimensional Jimbo–Miwa equation. *Chin. Phys. B* **2023**, *32*, 060201. [CrossRef]
19. Zhou, K.; Zhu, J.R.; Ren, B. Some Novel Fusion and Fission Phenomena for an Extended (2+1)-Dimensional Shallow Water Wave Equation. *Symmetry* **2024**, *16*, 82. [CrossRef]
20. Jin, X.W.; Lin, J. Rogue wave, interaction solutions to the KMM system. *J. Magn. Magn. Mater.* **2020**, *502*, 166590. [CrossRef]
21. Wu, J.W.; Deng, Y.J.; Lin, J. Interactions solutions of various-type rogue with multi-stripe solitons and breather lump for the (2+1)-dimensional Maccari's system. *Int. J. Mod. Phys. B* **2020**, *34*, 2050268. [CrossRef]
22. Chen, S.J.; Lü, X.; Li, M.G.; Wang, F. Derivation and simulation of the M-lump solutions to two (2+1)-dimensional nonlinear equations. *Phys. Scr.* **2021**, *96*, 095201. [CrossRef]

23. Li, Z.Q.; Chen, Q.Q.; Wang, M.M.; Li, B. New mixed solutions generated by velocity resonance in the (2+1)-dimensional Sawada–Kotera equation. *Nonlinear Dyn.* **2022**, *108*, 1617–1626.
24. Ma, W.X. Lump waves in a spatial symmetric nonlinear dispersive wave model in (2+1)-dimensions. *Mathematics* **2023**, *11*, 4664. [CrossRef]
25. Yan, X.W.; Chen, Y.; Wang, X.B.; Tian, S.F. General multi-breather, high-order lump and semi-rational solutions of the (2+1)-dimensional Mel'nikov equation. *J. Phys. Soc. Jpn.* **2024**, *92*, 024006. [CrossRef]
26. Holloway, P.E.; Pelinovsky, E.; Talipova, T.; Barnes, B. A nonlinear model of internal tide transformation on the Australian North West Shelf. *J. Phys. Oceanogr.* **1997**, *27*, 871–896. [CrossRef]
27. Yang, Y.; Gao, Y.X.; Yang, H.W. Analysis of the rogue waves in the blood based on the high-order NLS equations with variable coefficients. *Chin. Phys. B* **2021**, *30*, 110202. [CrossRef]
28. Gao, X.Y.; Guo, Y.J.; Shan, W.R. Beholding the shallow water waves near an ocean beach or in a lake via a Boussinesq-Burgers system. *Chaos Soliton Fract.* **2021**, *147*, 110875. [CrossRef]
29. Zhang, Y.C.; Zhao, M.; Sun, D.H.; Dong, C. An extended continuum mixed traffic model. *Nonlinear Dyn.* **2021**, *103*, 1891–1909. [CrossRef]
30. Bertini, L.; Giacomin, G. Stochastic Burgers and KPZ equations from particle systems. *Commun. Math. Phys.* **1997**, *183*, 571–607. [CrossRef]
31. Liu, X.Z.; Yu, J.; Ren, B.; Yang, J.R. Bäcklund transformations for the Burgers equation via localization of residual symmetries. *Chin. Phys. B* **2014**, *23*, 110203. [CrossRef]
32. Hu, H.C.; Li, Y.Y.; Zhu, H.D. Residual symmetry, interaction solutions and consistent tanh expansion solvability for the third-order Burgers equation. *Chaos Soliton Fract.* **2018**, *108*, 77–81. [CrossRef]
33. Yan, Z.W.; Lou, S.Y. Soliton molecules in Sharma–Tasso–Olver–Burgers equation. *Appl. Math. Lett.* **2020**, *104*, 106271. [CrossRef]
34. Lü, Z.S.; Zhang, H.Q. Soliton-like and period form solutions for high dimensional nonlinear evolution equations. *Chaos Soliton Fract.* **2003**, *17*, 669–673. [CrossRef]
35. Gao, C.N.; Wang, Y.H. Lump-type solutions, interaction solutions, and periodic lump solutions of the generalized (3+1)-dimensional Burgers equation. *Mod. Phys. Lett. B* **2021**, *35*, 2150107. [CrossRef]
36. Liu, J.; Wu, J.W. Lump and interaction solutions to the (3+1)-dimensional Burgers equation. *Chin. Phys. B* **2020**, *29*, 030201. [CrossRef]
37. Chen, S.J.; Lü, X.; Tang, X.F. Novel evolutionary behaviors of the mixed solutions to a generalized Burgers equation with variable coefficients. *Commun. Nonlinear Sci. Numer. Simulat.* **2021**, *95*, 105628. [CrossRef]
38. Holden, H.; Øksendal, B.; Ubøe, J.; Zhang, T. *Stochastic Partial Differential Equations*; Springer: Berlin/Heidelberg, Germany, 2010.
39. Wang, H.; Tian, S.F.; Chen, Y.; Zhang, T.T. Dynamics of kink solitary waves and lump waves with interaction phenomena in a generalized (3+1)-dimensional Kadomtsev–Petviashvili–Boussinesq equation. *Int. J. Comput. Math.* **2019**, *97*, 2178–2190. [CrossRef]
40. Kharif, C.; Pelinovsky, E.; Slunyaev, A. *Rogue Waves in the Ocean*; Springer: Berlin/Heidelberg, Germany, 2009.
41. Zhang, X.; Chen, Y. General high-order rogue waves to nonlinear Schrödinger–Boussinesq equation with the dynamical analysis. *Nonlinear Dyn.* **2018**, *93*, 2169–2184. [CrossRef]